DIAGNOSTIC NEURORADIOLOGY

CrossMark

Amide proton transfer-weighted MRI in distinguishing high- and low-grade gliomas: a systematic review and meta-analysis

Chong Hyun Suh[1] · Ji Eun Park[1] (iD) · Seung Chai Jung[1] · Choong Gon Choi[1] · Sang Joon Kim[1] · Ho Sung Kim[1]

Abstract

Purpose Grading of brain gliomas is of clinical importance, and noninvasive molecular imaging may help differentiate low- and high-grade gliomas. We aimed to evaluate the diagnostic performance of amide proton transfer-weighted (APTw) MRI for differentiating low- and high-grade gliomas on 3-T scanners.

Methods A systematic literature search of Ovid-MEDLINE and EMBASE was performed up to March 28, 2018. Original articles evaluating the diagnostic performance of APTw MRI for differentiating low- and high-grade gliomas were selected. The pooled sensitivity and specificity were calculated using a bivariate random-effects model. A coupled forest plot and a hierarchical summary receiver operating characteristic curve were obtained. Heterogeneity was investigated using Higgins inconsistency index (I^2) test. Meta-regression was performed.

Results Ten original articles with a total of 353 patients were included. High-grade gliomas showed significantly higher APT signal intensity than low-grade gliomas. The pooled sensitivity and specificity for the diagnostic performance of APTw MRI for differentiating low-grade and high-grade gliomas were 88% (95% CI, 77–94%) and 91% (95% CI, 82–96%), respectively. Higgins I^2 statistic demonstrated heterogeneity in the sensitivity ($I^2 = 68.17\%$), whereas no heterogeneity was noted in the specificity ($I^2 = 44.84\%$). In meta-regression, RF saturation power was associated with study heterogeneity. Correlation coefficients between APT signal intensity and Ki-67 cellular proliferation index ranged from 0.430 to 0.597, indicating moderate correlation. All studies showed excellent interobserver agreement.

Conclusions Although heterogeneous protocols were used, APTw MRI demonstrated excellent diagnostic performance for differentiating low- and high-grade gliomas. APTw MRI could be a reliable technique for glioma grading in clinical practice.

Keywords Glioma · Grading · Amide proton transfer · Chemical exchange saturation transfer

Abbreviations

CEST   Chemical exchange saturation transfer
APT   Amide proton transfer
PRISMA Preferred Reporting Items for Systematic Reviews and Meta-Analyses
QUADAS-2   Quality Assessment of Diagnostic Accuracy Studies-2
HSROC   Hierarchical summary receiver operating characteristic

✉ Ji Eun Park
  jieunp@gmail.com

[1] Department of Radiology and Research Institute of Radiology, University of Ulsan College of Medicine, Asan Medical Center, 43 Olympic-ro 88, Songpa-Gu, Seoul 05505, South Korea

Introduction

Glioma grading is of critical clinical importance, as the prognosis substantially differs according to the grade, as does the management strategy [1]. Amide proton transfer-weighted (APTw) MRI, which uses image contrast based on chemical exchange saturation transfer (CEST), could be a useful noninvasive technique for glioma grading, as it provides indirect measurements of mobile proteins and peptides [2–4]. Since high-grade gliomas are associated with increased expression of cellular proteins and peptides relative to low-grade glioma [5], APTw MRI may predict the cellular proliferation index [6–8] and differentiate low- from high-grade gliomas with higher diagnostic sensitivity and specificity compared to

current imaging methods [6–15]. APTw MRI was shown to have superior accuracy for differentiating tumor progression from treatment-related change compared with MR spectroscopy [12]. APTw MRI also has direct biologic relevance compared with cerebral blood volume and apparent diffusion coefficient measurements [9, 11].

To become a clinically useful biomarker, an imaging technique needs to present reliable estimates of disease status in different protocols and processing methods. Although APTw MRI is reported to be a potentially useful tool in pre- and post-treatment tumors [6–15], APTw MRI protocols are not yet standardized, and the CEST effect greatly depends on RF power, saturation time, pulse sequence, and other imaging parameters [16]. This study addresses whether variations in APTw MRI protocols and post-processing analysis have an impact on the diagnostic accuracy in differentiating low from high-grade gliomas. An additional goal of this meta-analysis is to increase the power of the statistics by aggregating data, as most of the studies investigating APTw MRI have a relatively small sample size.

Meta-analyses have systematically reviewed the clinical utility of advanced imaging techniques, such as diffusion-weighted imaging [17], perfusion-weighted imaging [18], magnetic resonance spectroscopy [19], and positron emission tomography [20], in the assessment of glioma grading. Since APTw MRI is a novel molecular imaging technique that has not yet been previously systematically reviewed in the evaluation of glioma grading, this study aims to assess the diagnostic accuracy of APTw MRI based on existing literature in determining the cellular proliferation index, differentiating between low and high grade gliomas, and confirming interobserver consistency in light of the various imaging protocols and post-processing analysis utilized in prior studies.

Materials and methods

This systematic review and meta-analysis followed the Preferred Reporting Items for Systematic Reviews and Meta-Analyses (PRISMA) guidelines [21].

Literature search

A computerized literature search using Ovid-MEDLINE and EMBASE up to March 28, 2018, was performed to identify articles assessing the diagnostic performance of APTw MRI for differentiating low-grade and high-grade gliomas. The following search terms were used: ((glioma) OR (oligodendroglioma) OR (astrocytoma) OR (glioblastoma) OR ("brain tumor")) AND ((amide proton transfer) OR (APT)). The search was not limited to articles in terms of English language, human or animal studies, or search date.

The bibliographies of relevant articles were also searched to expand the extent of the search.

Eligibility criteria

Articles were selected if all of the following inclusion criteria were satisfied: (a) patients with histopathologically confirmed gliomas; (b) patients who underwent pre-treatment APTw MRI; (c) a reference standard based on histopathology; and (d) sufficient data for the reconstruction of two by two tables for differentiating low-grade and high-grade gliomas.

Articles were excluded according to any of the following exclusion criteria: (a) conference abstracts; (b) reviews; (c) case reports or case series including fewer than 10 patients; (d) letters, editorials, or comments; (e) animal or phantom studies; and (f) articles with a partially overlapping patient cohort. For articles with a partially overlapping patient cohort, the study with the largest population was chosen. If a 2×2 table could not be obtained, the authors of the articles were contacted for provision of further data.

Data extraction and quality assessment

The literature search, literature selection, data extraction, and quality assessment were assessed independently by two reviewers (C.H.S. and J.E.P.). If disagreement was revealed, a third reviewer (H.S.K.) was consulted. Quality assessment of the selected studies was performed using the Quality Assessment of Diagnostic Accuracy Studies-2 (QUADAS-2) criteria [22].

The following data were extracted from the relevant studies using a standardized extraction form: (a) study characteristics: study institution, period of patient enrollment, study design, method of patient enrollment (consecutive or nonconsecutive), reference standard, and interval between APTw MRI and reference standard; (b) patient characteristics: total number of patients, number of patients with high-grade and low-grade gliomas, mean age, age range, and male to female ratio; (c) technical characteristics of MRI: magnetic field strength, vendor, model, head coil channels, data acquisition (three dimensional [3D] or two dimensional [2D]), APTw MRI sequences, TR (ms), TE (ms), number of saturation offsets (frequencies), power of radiofrequency (RF) saturation (μT), type of RF for CEST saturation (pulsed or continuous), RF saturation duration (total, ms), B0 inhomogeneity correction, total scan time, imaging analysis software, and other parameters; (d) MRI interpretation: number of readers, reader experience, and reader blindness to the reference standard; and (e) outcome: diagnostic performance (sensitivity and specificity) of APTw MRI for differentiating low-grade (WHO grade I and II) and high-grade (WHO grade III and IV) gliomas, cutoff values of parameters for differentiating low-grade and high-grade gliomas, mean values ± standard deviation (SD) of APT

signal intensity for low-grade and high-grade gliomas, correlation between APT signal intensity and cellular proliferation index (Ki-67), and interobserver agreement in APTw MRI. If the diagnostic performances of several APTw MRI parameters were separately reported, the performance values of the parameter showing the highest performance were chosen.

Data synthesis and analysis

The pooled sensitivity and pooled specificity and their 95% CIs were obtained using a bivariate random-effects model [23–27]. The diagnostic odds ratio (DOR), pooled positive likelihood ratio (PLR), and negative likelihood ratio (NLR) were also obtained. The DOR was defined as the odds of having a positive APTw MRI result in patients with high-grade gliomas compared with the odds of having a positive APTw MRI result in patients without high-grade gliomas.

$$DOR = \frac{\text{True positive} \times \text{True negative}}{\text{False positive} \times \text{False negative}}$$

PLR was defined as the likelihood that an APTw MRI result positive for differentiating low-grade and high-grade gliomas would occur in patients with high-grade gliomas.

$$PLR = \frac{\text{Sensitivity}}{1 - \text{Specificity}}$$

NLR was defined as the likelihood that an APTw MRI result negative for differentiating low-grade and high-grade gliomas would occur in patients without high-grade gliomas.

$$NLR = \frac{1 - \text{Sensitivity}}{\text{Specificity}}$$

A coupled forest plot of sensitivity and specificity and a hierarchical summary receiver operating characteristic (HSROC) curve with 95% confidence and prediction regions were obtained.

Heterogeneity across the selected studies was investigated as follows: (a) Cochran's Q test with $p < 0.05$ taken to indicate the presence of heterogeneity; (b) Higgins inconsistency index (I^2) test with a value $> 50\%$ indicating the presence of heterogeneity [28]; (c) visual assessment of the coupled forest plot to assess the presence of a threshold effect (i.e., a positive correlation between sensitivity and false positive rate among the included studies); (d) a Spearman correlation coefficient between the sensitivity and false positive rate > 0.6, which also indicates a threshold effect [29]; and (e) visual assessment of the HSROC curve to evaluate the difference between the 95% confidence and prediction regions, with a large difference indicating heterogeneity.

A Deeks' funnel plot was performed to evaluate publication bias, with statistical significance being assessed by

Deeks' asymmetry test [30]. A meta-regression was conducted to explain the effects of heterogeneity, with the following covariates being evaluated using a bivariate model: (a) study design (prospective vs. retrospective); (b) MRI vendor; (c) power of RF saturation (2 μT vs. 1 μT); and (d) data acquisition (3D vs. 2D). Data analyses were performed by one of the authors (C.H.S., with 5 years of experience in performing systematic reviews and meta-analyses) using the "Metandi" and "Midas" modules in Stata 15.0 (StataCorp, College Station, TX) and the "Mada" package in R version 3.4.1 (R Foundation for Statistical Computing, Vienna, Austria). A value of $p < 0.05$ was considered as indicating statistical significance.

Results

Literature selection

The detailed literature selection process is shown in Fig. 1. The computerized literature search returned 186 articles from Ovid-MEDLINE ($n = 92$) and EMBASE ($n = 94$). After removal of 10 duplicates, screening of the titles and abstracts of the 176 remaining articles was conducted, and 151 articles were excluded as follows: 81 articles were not in the field of interest, 33 conference abstracts, 25 reviews, 11 case reports, and 1 letter. Full-text reviews of the 25 potentially eligible articles were carefully performed, and 15 articles were excluded (Supplementary materials). Two articles included patients who enrolled during overlapping time periods from the same institution, we checked the authors and the patients were not overlapped [11, 12]. Finally, 10 original articles covering a total of 353 patients were included [6–15].

Characteristics of the included studies

The characteristics of the included studies are described in Table 1. Four of ten studies had a prospective design [7, 8, 10, 15], three studies had a retrospective design [9, 11, 12], and the other studies did not report the design. Patient enrollment was conducted in a consecutive manner in six studies [7–9, 11–13], while the enrollment process was not reported in the other studies [6, 10, 14, 15]. Histopathology was used as the reference standard in all studies, as this formed one of the inclusion criteria.

The detailed parameters of the different APTw MRI sequences are described in Table 2. APTw MRI was performed using a 3D acquisition in five studies [9–12, 14] and a 2D acquisition in five studies [6–8, 13, 15]. A gradient echo sequence was used in four studies [6, 7, 11, 12], a spin echo sequence in three studies [8, 13, 15], and

Fig. 1 PRISMA flow diagram of the study selection process
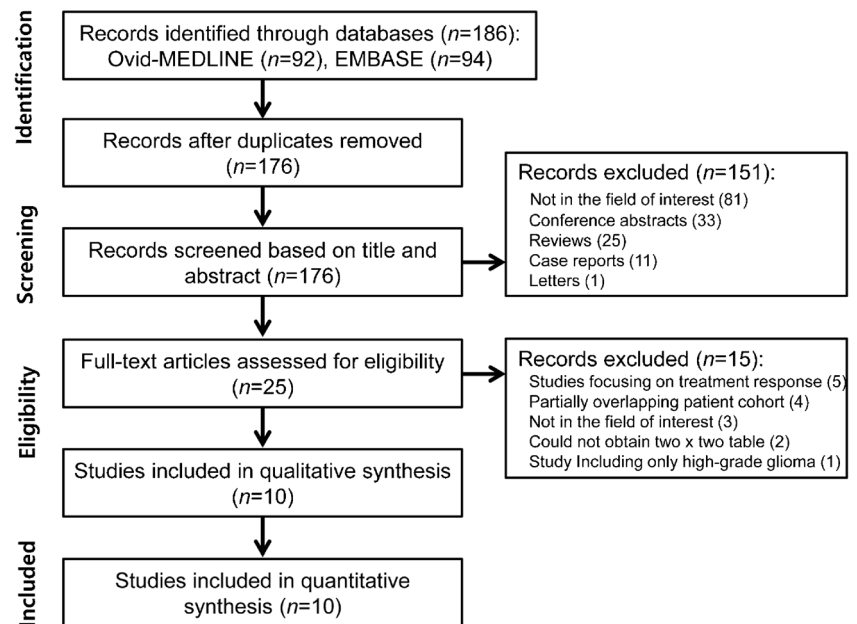
gradient and spin echo sequences in three studies [9, 10, 14]. Various saturation offsets and frequencies were used, with a RF saturation pulse power of 2 μT being used in seven studies [6–10, 14, 15], and 1 μT in three studies [11–13]. In all studies, the magnetization transfer ratio asymmetry (MTR_{asym}) values were calculated at an offset of 3.5 ppm, the so-called APT-weighted signal values.

Image postprocessing was performed using Interactive Data Language in four studies [6, 10, 14, 15], Matlab in four studies [9, 11–13], and ImageJ in one study [8]. In all studies, two or three neuroradiologists placed the regions of interest (ROIs) representing the solid component of the tumor on the APT map. Total acquisition time varied considerably, from 3 min 12 s to 10 min 42 s.

Table 1 Characteristics of the included studies

Author (year of publication)	Institution	Study period	No. of patients (n)	High-grade glioma (n)	Low-grade glioma (n)	Mean age (years)	Age range (years)	Male/ female
Bai Y, et al. [6] (2017)	Zhengzhou University People's Hospital and Henan Provincial People's Hospital, China	2012.8–2015.11	34	16	18	NA	NA	NA
Choi YS, et al. [9] (2017)	Yonsei University College of Medicine, South Korea	2014.11–2015.8	46	31	15	44.2	NA	25:21
Jiang, S et al. [10] (2017)	Johns Hopkins University, USA	2010.4–2015.3	24	13	11	50.5	NA	17:7
Park JE, et al. [11] (2015)	Asan Medical Center, South Korea	2013.8–2014.6	45	26	19	43.7	25–75	25:20
Park JE, et al. [12] (2016)	Asan Medical Center, South Korea	2014.5–2014.11	40	29	11	49.4	NA	23:17
Sakata A, et al. [13] (2017)	Kyoto University Graduate School of Medicine, Japan	2013.5–2014.8	21	11	10	50	11–85	13:8
Su C, et al. [7] (2017)	Tongji Hospital, China	2015.6–2016.1	42	14	28	42.2	NA	28:14
Togao O, et al. [8] (2014)	Kyushu University, Japan	NA	36	28	8	48.1	NA	16:20
Zhou J, et al. [14] (2013)	Johns Hopkins University, USA	NA	14	8	6	46.5 (median)	25–82	10:4
Zou T, et al. [15] (2018)	Zhujiang Hospital, China	2015.7–2016.6	51	26	25	40.9	18–63	30:21

APT amide proton transfer, *RF* radiofrequency, *NA* not available

Table 2 Amide proton transfer (APT)-weighted magnetic resonance imaging parameters

Author (year of publication)	MRI vendor	MRI scanner	Head coil (channel)	Data acquisition	Sequence	TR (ms)	TE (ms)	Number of saturation offsets (frequencies)	Power of RF saturation (μT)	Pulsed or continuous	RF saturation duration (total, ms)	MTR_{asym} (ppm)	B0 inhomogeneity correction	Total acquisition time
Bai Y, et al. [6] (2017)	Siemens	3-T Magnetom Trio	12	2D	Gradient echo	3200	2.87	21 (-5 to 5 ppm with a step size of 0.5 ppm)	2	Pulsed	995 (each 99 ms, gap 100 ms)	3.5	Train of 5 Gaussian-shaped RF	3 min 30 s
Choi YS, et al. [9] (2017)	Philips	3-T Achieva	32	3D	Gradient and spin echo	3000	17	6 (±3.0, ±3.5, and ±4.0 ppm)	2	Pulsed	800 (each 200 ms, no gap, a four block)	3.5	WASSR 21 offsets from 1.25 ppm to 1.25 ppm	7 min 36 s
Jiang, S et al. [10] (2017)	Philips	3-T Achieva	32	3D	Gradient and spin echo	3000	17	6 (±3.0, ±3.5, and ±4.0 ppm)	2	Pulsed	800 (each 200 ms, no gap, a four block)	3.5	WASSR 21 offsets from 1.25 ppm to 1.25 ppm	10 min 42 s
Park JE, et al. [11] (2015)	Philips	3-T Achieva	32	3D	Gradient echo	140	7.1	29 (-5 to 5 ppm with a step size of 0.36 ppm)	1	Pulsed	140 (each 70 ms, no gap)	3.5	Point-by-point delta B0 correction	8 min 50 s
Park JE, et al. [12] (2016)	Philips	3-T Achieva	32	3D	Gradient echo	140	7.1	29 (-5 to 5 ppm with a step size of 0.36 ppm)	1	Pulsed	140 (each 70 ms, no gap)	3.5	Point-by-point delta B0 correction	8 min 50 s
Sakata A, et al. [13] (2017)	Toshiba	3-T Vantage	32	2D	Fast spin echo	9000	60	40 (-10 to 10 ppm with a step size of 0.5 ppm)	1	Pulsed	NA (each 25 ms, gap 1 ms)	between 3.3 and 3.7	Point-by-point delta B0 correction	6 min 9 s
Su C, et al. [7] (2017)	GE	3-T Discovery MR750	NA	2D	Gradient echo	3000	22.6	64 (±6, ±5, ±4.5, ±4, ±3.75, ±3.5, ±3.25, ±3, ±2.5, ±2, ±1.5, ±1, ±0.75, ±0.5, ±0.25, and 0 ppm)	2	Pulsed	400 (each 400 ms)	3.5	Shifting the minimum signal of the z-spectrum to 0 Hz	3 min 18 s
Togao O, et al. [8] (2014)	Philips	3-T Achieva TX	8	2D	Spin echo	5000	6	25 (-6 to 6 ppm with a step size of 0.5 ppm)	2	Pulsed	2000 (each 50 ms, 40×50 ms, sinc-gauss-shaped elements)	3.5	2D gradient echo, a point-by-point delta B0 correction	2 min 20 s for one z-spectrum
Zhou J, et al. [14] (2013)	Philips	3-T Achieva	32	3D	Gradient and spin echo	3000	17	6 (±3.0, ±3.5, and ±4.0 ppm)	2	Pulsed	800 (each 200 ms, no gap, a four block)	3.5	WASSR 24 offsets from 1.5 ppm to 1.5 ppm	10 min 42 s
Zou T, et al. [15] (2018)	Philips	3-T Achieva	16	2D	Turbo spin echo	3000	11	31 offsets: 0, ±0.25, ±0.5, ±0.75, ±1, ±1.5, ±2, ±2.5, ±3 (2), ±3.25 (4), ±3.5 (8), ±3.75 (4), ±4 (2), ±4.5, ±5, ±6 ppm 31 (0, ±0.25, ±0.5, ±0.75, ±1, ±1.5, ±2, ±2.5, ±3, ±3.25, ±3.5, ±3.75, ±4, ±4.5, ±5, and ±6 ppm)	2	Pulsed	800 (each 200 ms × 4, interpulse delay 10 ms)	3.5	NA	3 min 12 s

RF radiofrequency, MTR_{asym} asymmetric magnetization transfer ratio, *WASSR* water saturation shift referencing method, *NA* not available

Quality assessment

The quality of the included studies was considered moderate, with 8 of the 10 studies satisfying at least 4 of the 7 QUADAS-2 domains (Supplementary Fig. 1). In terms of the index test domain, seven studies were considered to have an unclear risk of bias because it was unclear whether APTw MRI was interpreted blinded to the reference standard [10, 12, 9, 11, 13–15]. In addition, in the reference standard domain, nine studies were considered to have an unclear risk of bias as it was not clear whether the reference standard was interpreted blinded to the APTw MRI [6–13, 15]. However, we considered that this issue was not related to the applicability of the studies.

Diagnostic performance of APTw MRI for glioma grading

APT signal intensity (%) was used as the main parameter in all studies. APT_{90} (90% histogram cutoffs for APT values) was used in three studies [11–13], and APT_{max} (maximum signal intensity of APT) was used in one study [10]. In all studies, as the glioma grade increased, the APT signal intensity also increased. High-grade gliomas demonstrated significantly higher APT signal intensity than low-grade gliomas (Table 3). Cutoff values for APT signal intensity varied from 1.53 to 3.70%, with the median cutoff value being 2.23%. The

sensitivities of the individual studies varied from 62 to 100%, and the specificities varied from 71 to 100%.

The pooled sensitivity and specificity for the diagnostic performance of APTw MRI for differentiating low-grade and high-grade gliomas were 88% (95% CI, 77–94%) and 91% (95% CI, 82–96%), respectively (Fig. 2). The pooled DOR, PLR, and NLR were 73 (95% CI, 24–222), 9.5 (95% CI, 4.6–19.5), and 0.13 (95% CI, 0.06–0.26), respectively. The area under the HSROC curve was 0.95 (95% CI, 0.93–0.97).

The Q test showed that heterogeneity was absent ($Q = 4.328$, $p = 0.057$), but the Higgins I^2 test demonstrated that heterogeneity was present in the sensitivity ($I^2 = 68.17\%$), but not in the specificity ($I^2 = 44.84\%$). There was no evidence of a threshold effect in the coupled forest plot (Fig. 3). The Spearman correlation coefficient was −0.081 (95% CI, −0.676–0.578), which also indicates no threshold effect. In the HSROC curve, there was a large difference between the 95% confidence and prediction regions, which indicates the possibility of heterogeneity (Fig. 3). The Deeks' funnel plot revealed that the likelihood of publication bias was low ($p = 0.81$; Supplementary Fig. 2).

Meta-regression

A meta-regression was performed to explain the effects of heterogeneity (Supplementary Table 1). Among the potential covariates, the power of the RF saturation was associated with

Table 3 Outcomes of the included studies

Author (year of publication)	APTw MRI parameter (%)	Cutoff value (%)	APT signal intensity for low-grade glioma (% ± SD)	APT signal intensity for high-grade glioma (% ± SD)	Correlation coefficient with Ki-67	Intraclass correlation coefficient (95% CI)
Bai Y, et al. [6] (2017)	APT signal intensity	NA	1.3 ± 0.2	2.1 ± 0.2	0.597	0.919 (NA)
Choi YS, et al. [9] (2017)	APT signal intensity	1.53	0.8 ± 0.6	2.2 ± 0.9	NA	0.96 (0.93–0.98)
Jiang S, et al. [10] (2017)	APT_{max} (maximum signal intensity of APT)	2.74	2.1 (95% CI, 1.7–2.4)	3.3 (95% CI, 3.0–3.8)	0.538	NA
Park JE, et al. [11] (2015)	APT_{90} (90% histogram cutoffs for APT)	3.70	2.3 ± 0.8	4.0 ± 1.2	NA	0.89 (NA)
Park JE, et al. [12] (2016)	APT_{90} (90% histogram cutoffs for APT)	1.72	1.1 ± 0.9	2.9 ± 1.6	NA	0.95
Sakata A, et al. [13] (2017)	APT signal intensity	2.72	NA	NA	NA	Cohen's kappa, 1
Su C, et al. [7] (2017)	APT signal intensity	3.11 or 2.8	2.7 ± 0.2	3.7 ± 0.2	0.502	0.94 (0.89–0.96)
Togao O, et al. [8] (2014)	APT signal intensity	2.54	2.1 ± 0.4	3.8 ± 1.0	0.430	0.81 (NA)
Zhou J, et al. [14] (2013)	APT signal intensity	NA	NA	NA	NA	NA
Zou T, et al. [15] (2018)	APT signal intensity	2.34	2.0 ± 0.6	2.8 ± 0.4	NA	Cronbach alpha, 0.984; standardized Cronbach alpha, 0.986

APTw MRI amide proton transfer-weighted magnetic resonance imaging, *SD* standard deviation, *CI* confidence interval, *NA* not available
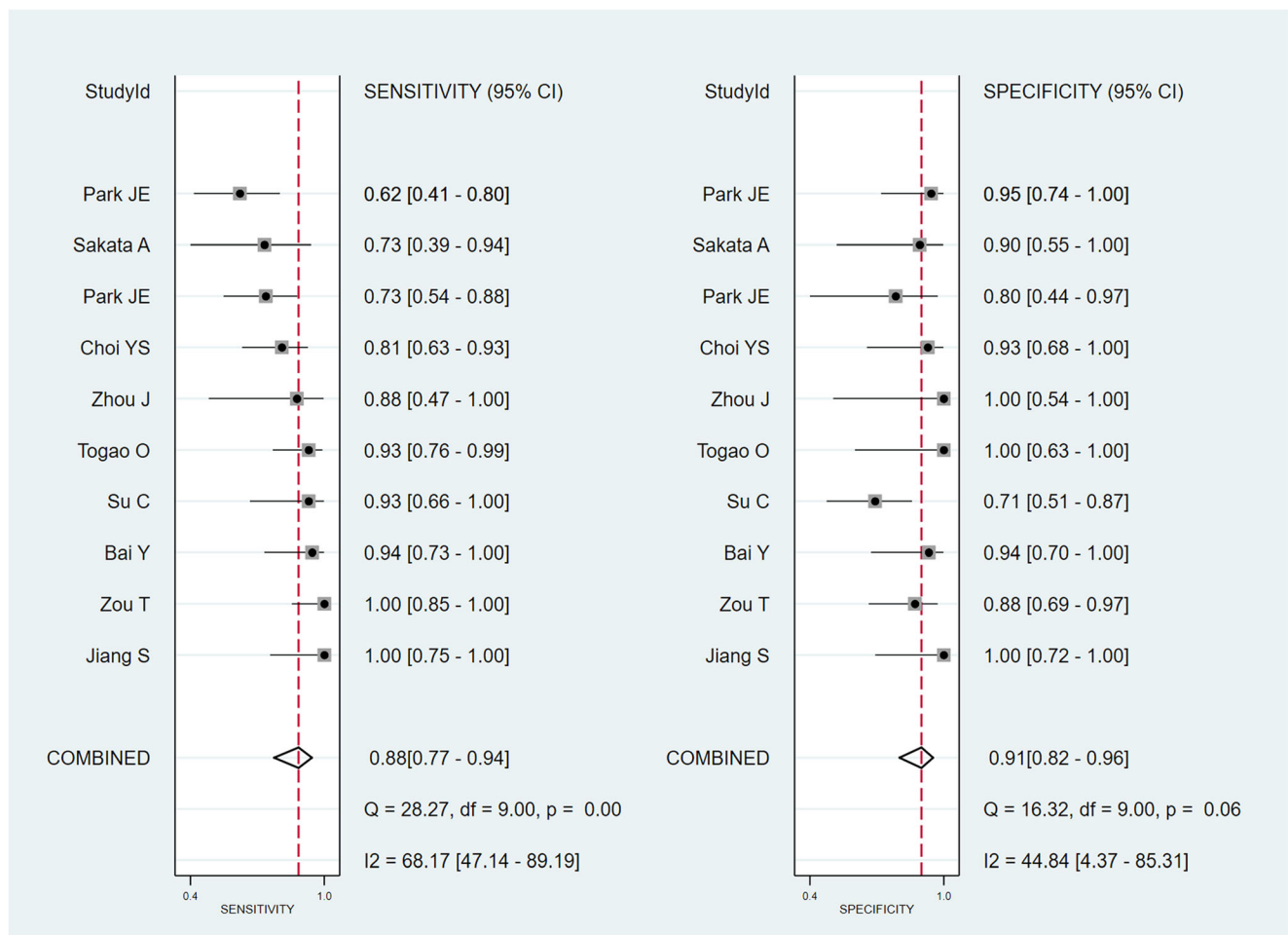
Fig. 2 Coupled forest plots of sensitivity and specificity for the diagnostic performance of APTw MRI for glioma grading. Horizontal lines indicate 95% CIs

study heterogeneity. Studies using a 2-μT RF saturation power showed significantly higher sensitivity (92% [95% CI, 87–97%]) than studies using 1 μT (69% [95% CI, 56–81%]). Otherwise, the study design, MRI vendor, and data acquisition (3D or 2D) covariates did not significantly affect study heterogeneity.

Correlation between APT signal intensity and Ki-67

Four studies evaluated the correlation between APT signal intensity and Ki-67 (Table 3) [6–8, 10]. The correlation coefficients ranged from 0.430 to 0.597, indicating moderate correlations between APT signal intensity and Ki-67.

Interobserver agreement

Among the 10 studies, 8 evaluated interobserver agreement for quantitative APTw MRI parameters (Table 3) [6–9, 11–13, 15]. Six studies used intraclass correlation coefficient (ICC) [6–9, 11, 12], one study used Cohen's kappa [13], and one study used Cronbach alpha and standardized Cronbach alpha

[15]. All studies showed excellent interobserver agreement (ICC, 0.81–0.95; Cohen's kappa, 1; Cronbach alpha, 0.984; and standardized Cronbach alpha, 0.986).

Discussion

This meta-analysis systematically reviewed the diagnostic accuracy of APTw MRI in grading gliomas, the correlation between APT signal intensity and Ki-67 and the interobserver agreement in interpreting APTw MRI based on 10 studies and 363 patients. High-grade gliomas showed significantly higher APT signal intensity than low-grade gliomas. The pooled sensitivity was 88% (95% CI, 77–94%), the pooled specificity was 91% (95% CI, 82–96%), and the area under the HSROC curve was 0.95 (95% CI, 0.93–0.97). In addition, the correlation between APT signal intensity and Ki-67 was moderate, and the interobserver agreement for APTw MRI was excellent. Although the protocols used at 3-T were heterogeneous, APTw MRI demonstrated excellent diagnostic performance for differentiating low-grade and high-grade gliomas,
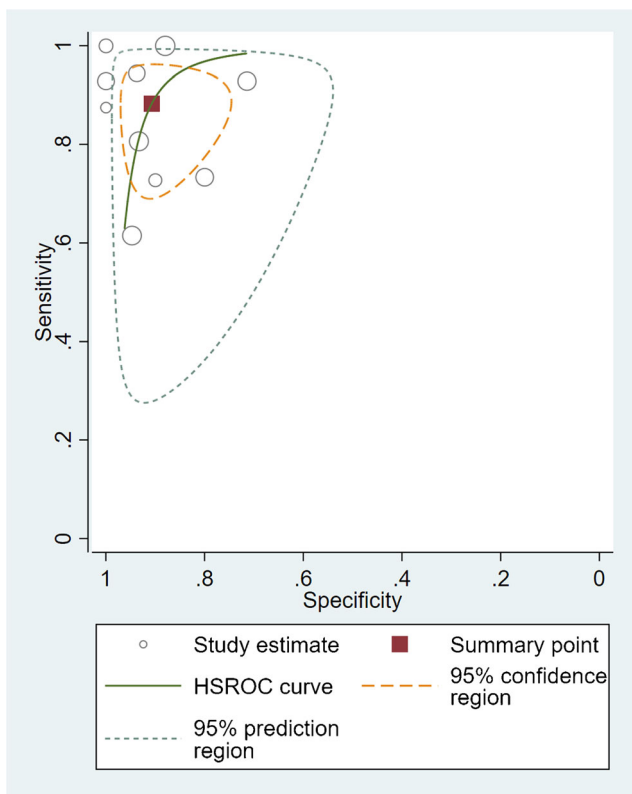
Fig. 3 Hierarchical summary receiver operating characteristic (HSROC) curve of the diagnostic performance of APTw MRI for glioma grading

suggesting that APTw MRI could be a reliable technique for glioma grading in clinical practice.

APTw MRI offers several advantages for brain tumor imaging. First, APTw MRI is a noninvasive technique, and because the contrast is based on endogenous amide protons, the administration of a contrast agent is not needed [9]. Therefore, APTw MRI is particularly helpful if the condition of the patient contraindicates the use of a contrast agent injection. Second, APTw MRI is a reliable method for obtaining quantitative APT parameters, with our results showing excellent interobserver agreement for APTw MRI (ICC, 0.81–0.94). Third, APTw MRI may reflect cellular proliferation, because abnormal protein synthesis causes overexpression of various proteins and peptides [31]. Our study results revealed moderate correlations between APT signal intensity and Ki-67.

This study highlights the importance of technical considerations for APTw MRI. The increased APT signal intensity at the higher RF power might have enhanced the diagnostic value of APTw MRI. All studies applied pulsed RF saturation, but other parameters including pulse sequences, numbers of saturation offsets and frequencies, duration of saturation, and data analysis methods varied between the studies. A previous report demonstrated that different analytical approaches influenced on APT signal intensities [32]. The results of this study emphasize that the imaging protocols, post-processing analysis, and APT signal intensity values need to be standardized

across institutions before becoming clinically viable. Continuous efforts to standardize protocols are required, both from vendors and researchers.

Several clinical applications of APTw MRI in brain tumors should be noted. First, APTw MRI can accurately differentiate high-grade gliomas from low-grade gliomas. This study reviewing all currently available articles demonstrated that APTw MRI had high diagnostic performance for differentiating low-grade and high-grade glioma. Second, APTw MRI could be used to evaluate treatment response in pre- and post-treatment gliomas. Previous studies showed that APTw MRI demonstrated high performance for evaluating treatment response in newly diagnosed glioblastoma [33] and post-treatment glioma [12, 34]. Third, APTw MRI shows promising results for differentiating malignant brain tumors (including metastasis) from glioblastoma [35], and primary central nervous system lymphoma from high-grade glioma [36]. Last but not least, APTw MRI could assist tissue biopsy by increasing the accuracy of tumor sampling in patients with infiltrating gliomas [10]. APTw MRI is currently gaining interest, and its technical validation and clinical validation are ongoing. Further clinical validations for various clinical applications are warranted.

Aside from its small sample size, this study is subject to several other limitations. First, the studies included here used pulsed RF saturation, while recent advances in APTw MRI have enabled continuous RF saturation at 3 T [37, 38]. Updating the findings with studies using this recent technique will be desirable in a future meta-analysis. Second, while the I^2 test revealed heterogeneity for sensitivity, the power of this test is low given the small number of studies included. We performed meta-regression and found that the power of the RF saturation was associated with study heterogeneity. Third, while the funnel plot did not appear to reveal any publication bias, it should be interpreted with caution given the low number of studies included. Further evaluation of the effects of pH, nuclear Overhauser effect, magnetization transfer effect, water content, temperature, and T1 values of water protons need to be addressed.

In conclusion, although the 3-T protocols used for APTw MRI were heterogenous, the technique demonstrated excellent diagnostic performance for differentiating low-grade from high-grade glioma. APTw MRI could be a reliable technique for glioma grading in clinical practice.

Compliance with ethical standards

Conflict of interest The authors declare that they have no conflict of interest.

Ethical approval All procedures performed in the studies involving human participants were in accordance with the ethical standards of the institutional and/or national research committee and with the 1964 Helsinki Declaration and its later amendments or comparable ethical standards.

Informed consent Informed consent was obtained from all individual participants included in the meta-analysis studies.

Publisher's note Springer Nature remains neutral with regard to jurisdictional claims in published maps and institutional affiliations.

References

1. Louis DN, Ohgaki H, Wiestler OD, Cavenee WK, Burger PC, Jouvet A, Scheithauer BW, Kleihues P (2007) The 2007 WHO classification of tumours of the central nervous system. Acta Neuropathol 114:97–109. https://doi.org/10.1007/s00401-007-0243-4

2. Zhou J, Lal B, Wilson DA, Laterra J, van Zijl PC (2003) Amide proton transfer (APT) contrast for imaging of brain tumors. Magn Reson Med 50:1120–1126. https://doi.org/10.1002/mrm.10651

3. Jones CK, Schlosser MJ, van Zijl PC, Pomper MG, Golay X, Zhou J (2006) Amide proton transfer imaging of human brain tumors at 3T. Magn Reson Med 56:585–592. https://doi.org/10.1002/mrm.20989

4. van Zijl PC, Yadav NN (2011) Chemical exchange saturation transfer (CEST): what is in a name and what isn't? Magn Reson Med 65:927–948. https://doi.org/10.1002/mrm.22761

5. Wen Z, Hu S, Huang F, Wang X, Guo L, Quan X, Wang S, Zhou J (2010) MR imaging of high-grade brain tumors using endogenous protein and peptide-based contrast. NeuroImage 51:616–622. https://doi.org/10.1016/j.neuroimage.2010.02.050

6. Bai Y, Lin Y, Zhang W, Kong L, Wang L, Zuo P, Vallines I, Schmitt B, Tian J, Song X, Zhou J, Wang M (2017) Noninvasive amide proton transfer magnetic resonance imaging in evaluating the grading and cellularity of gliomas. Oncotarget 8:5834–5842. https://doi.org/10.18632/oncotarget.13970

7. Su C, Liu C, Zhao L, Jiang J, Zhang J, Li S, Zhu W, Wang J (2017) Amide proton transfer imaging allows detection of glioma grades and tumor proliferation: comparison with Ki-67 expression and proton MR spectroscopy imaging. AJNR Am J Neuroradiol 38:1702–1709. https://doi.org/10.3174/ajnr.A5301

8. Togao O, Yoshiura T, Keupp J, Hiwatashi A, Yamashita K, Kikuchi K, Suzuki Y, Suzuki SO, Iwaki T, Hata N, Mizoguchi M, Yoshimoto K, Sagiyama K, Takahashi M, Honda H (2014) Amide proton transfer imaging of adult diffuse gliomas: correlation with histopathological grades. Neuro-Oncology 16:441–448. https://doi.org/10.1093/neuonc/not158

9. Choi YS, Ahn SS, Lee SK, Chang JH, Kang SG, Kim SH, Zhou J (2017) Amide proton transfer imaging to discriminate between low- and high-grade gliomas: added value to apparent diffusion coefficient and relative cerebral blood volume. Eur Radiol 27:3181–3189. https://doi.org/10.1007/s00330-017-4732-0

10. Jiang S, Eberhart CG, Zhang Y, Heo HY, Wen Z, Blair L, Qin H, Lim M, Quinones-Hinojosa A, Weingart JD, Barker PB, Pomper MG, Laterra J, van Zijl PCM, Blakeley JO, Zhou J (2017) Amide proton transfer-weighted magnetic resonance image-guided stereotactic biopsy in patients with newly diagnosed gliomas. Eur J Cancer 83:9–18. https://doi.org/10.1016/j.ejca.2017.06.009

11. Park JE, Kim HS, Park KJ, Choi CG, Kim SJ (2015) Histogram analysis of amide proton transfer imaging to identify contrast-enhancing low-grade brain tumor that mimics high-grade tumor: increased accuracy of MR perfusion. Radiology 277:151–161. https://doi.org/10.1148/radiol.2015142347

12. Park JE, Kim HS, Park KJ, Kim SJ, Kim JH, Smith SA (2016) Pre- and posttreatment glioma: comparison of amide proton transfer imaging with MR spectroscopy for biomarkers of tumor proliferation. Radiology 278:514–523. https://doi.org/10.1148/radiol.2015142979

13. Sakata A, Fushimi Y, Okada T, Arakawa Y, Kunieda T, Minamiguchi S, Kido A, Sakashita N, Miyamoto S, Togashi K (2017) Diagnostic performance between contrast enhancement, proton MR spectroscopy, and amide proton transfer imaging in patients with brain tumors. J Magn Reson Imaging 46:732–739. https://doi.org/10.1002/jmri.25597

14. Zhou J, Zhu H, Lim M, Blair L, Quinones-Hinojosa A, Messina SA, Eberhart CG, Pomper MG, Laterra J, Barker PB, van Zijl PCM, Blakeley JO (2013) Three-dimensional amide proton transfer MR imaging of gliomas: initial experience and comparison with gadolinium enhancement. J Magn Reson Imaging 38:1119–1128. https://doi.org/10.1002/jmri.24067

15. Zou T, Yu H, Jiang C, Wang X, Jiang S, Rui Q, Mei Y, Zhou J, Wen Z (2018) Differentiating the histologic grades of gliomas preoperatively using amide proton transfer-weighted (APTW) and intravoxel incoherent motion MRI. NMR Biomed 31:e3850. https://doi.org/10.1002/nbm.3850

16. Wu B, Warnock G, Zaiss M, Lin C, Chen M, Zhou Z, Mu L, Nanz D, Tuura R, Delso G (2016) An overview of CEST MRI for non-MR physicists. EJNMMI Phys 3:19. https://doi.org/10.1186/s40658-016-0155-2

17. Zhang L, Min Z, Tang M, Chen S, Lei X, Zhang X (2017) The utility of diffusion MRI with quantitative ADC measurements for differentiating high-grade from low-grade cerebral gliomas: evidence from a meta-analysis. J Neurol Sci 373:9–15. https://doi.org/10.1016/j.jns.2016.12.008

18. Delgado AF, Delgado AF (2017) Discrimination between glioma grades II and III using dynamic susceptibility perfusion MRI: a meta-analysis. AJNR Am J Neuroradiol 38:1348–1355. https://doi.org/10.3174/ajnr.A5218

19. Wang Q, Zhang H, Zhang J, Wu C, Zhu WJ, Li FY, Chen XL, Xu BN (2016) The diagnostic performance of magnetic resonance spectroscopy in differentiating high-from low-grade gliomas: a systematic review and meta-analysis. Eur Radiol 26:2670–2684. https://doi.org/10.1007/s00330-015-4046-z

20. Dunet V, Pomoni A, Hottinger A, Nicod-Lalonde M, Prior JO (2016) Performance of 18F-FET versus 18F-FDG-PET for the diagnosis and grading of brain tumors: systematic review and meta-analysis. Neuro-Oncology 18:426–434. https://doi.org/10.1093/neuonc/nov148

21. Liberati A, Altman DG, Tetzlaff J, Mulrow C, Gøtzsche PC, Ioannidis JP, Clarke M, Devereaux PJ, Kleijnen J, Moher D (2009) The PRISMA statement for reporting systematic reviews and meta-analyses of studies that evaluate health care interventions: explanation and elaboration. Ann Intern Med 151:W65–W94

22. Whiting PF, Rutjes AW, Westwood ME, Mallett S, Deeks JJ, Reitsma JB, Leeflang MM, Sterne JA, Bossuyt PM, QUADAS-2 Group (2011) QUADAS-2: a revised tool for the quality assessment of diagnostic accuracy studies. Ann Intern Med 155:529–536. https://doi.org/10.7326/0003-4819-155-8-201110180-00009

23. Suh CH, Park SH (2016) Successful publication of systematic review and meta-analysis of studies evaluating diagnostic test accuracy. Korean J Radiol 17:5–6. https://doi.org/10.3348/kjr.2016.17.1.5

24. Kim KW, Lee J, Choi SH, Huh J, Park SH (2015) Systematic review and meta-analysis of studies evaluating diagnostic test accuracy: a practical review for clinical researchers-part I. general guidance and tips. Korean J Radiol 16:1175–1187. https://doi.org/10.3348/kjr.2015.16.6.1175

25. Lee J, Kim KW, Choi SH, Huh J, Park SH (2015) Systematic review and meta-analysis of studies evaluating diagnostic test

accuracy: a practical review for clinical researchers-part II. Statistical methods of meta-analysis. Korean J Radiol 16:1188–1196. https://doi.org/10.3348/kjr.2015.16.6.1188

26. Reitsma JB, Glas AS, Rutjes AW, Scholten RJ, Bossuyt PM, Zwinderman AH (2005) Bivariate analysis of sensitivity and specificity produces informative summary measures in diagnostic reviews. J Clin Epidemiol 58:982–990. https://doi.org/10.1016/j.jclinepi.2005.02.022

27. Rutter CM, Gatsonis CA (2001) A hierarchical regression approach to meta-analysis of diagnostic test accuracy evaluations. Stat Med 20:2865–2884

28. Higgins JP, Thompson SG, Deeks JJ, Altman DG (2003) Measuring inconsistency in meta-analyses. BMJ 327:557–560. https://doi.org/10.1136/bmj.327.7414.557

29. Deville WL, Buntinx F, Bouter LM et al (2002) Conducting systematic reviews of diagnostic studies: didactic guidelines. BMC Med Res Methodol 2:9

30. Deeks JJ, Macaskill P, Irwig L (2005) The performance of tests of publication bias and other sample size effects in systematic reviews of diagnostic test accuracy was assessed. J Clin Epidemiol 58:882–893. https://doi.org/10.1016/j.jclinepi.2005.01.016

31. Cairns RA, Harris IS, Mak TW (2011) Regulation of cancer cell metabolism. Nat Rev Cancer 11:85–95. https://doi.org/10.1038/nrc2981

32. Sakata A, Okada T, Yamamoto A, Kanagaki M, Fushimi Y, Okada T, Dodo T, Arakawa Y, Schmitt B, Miyamoto S, Togashi K (2015) Grading glial tumors with amide proton transfer MR imaging: different analytical approaches. J Neuro-Oncol 122:339–348. https://doi.org/10.1007/s11060-014-1715-8

33. Park KJ, Kim HS, Park JE, Shim WH, Kim SJ, Smith SA (2016) Added value of amide proton transfer imaging to conventional and perfusion MR imaging for evaluating the treatment response of newly diagnosed glioblastoma. Eur Radiol 26:4390–4403. https://doi.org/10.1007/s00330-016-4261-2

34. Park JE, Lee JY, Kim HS, Oh JY, Jung SC, Kim SJ, Keupp J, Oh M, Kim JS (2018) Amide proton transfer imaging seems to provide higher diagnostic performance in post-treatment high-grade gliomas than methionine positron emission tomography. Eur Radiol 28:3285–3295. https://doi.org/10.1007/s00330-018-5341-2

35. Yu H, Lou H, Zou T, Wang X, Jiang S, Huang Z, du Y, Jiang C, Ma L, Zhu J, He W, Rui Q, Zhou J, Wen Z (2017) Applying protein-based amide proton transfer MR imaging to distinguish solitary brain metastases from glioblastoma. Eur Radiol 27:4516–4524. https://doi.org/10.1007/s00330-017-4867-z

36. Jiang S, Yu H, Wang X, Lu S, Li Y, Feng L, Zhang Y, Heo HY, Lee DH, Zhou J, Wen Z (2016) Molecular MRI differentiation between primary central nervous system lymphomas and high-grade gliomas using endogenous protein-based amide proton transfer MR imaging at 3 tesla. Eur Radiol 26:64–71. https://doi.org/10.1007/s00330-015-3805-1

37. Keupp J, Baltes C, Harvey P, Van den Brink J (2011) Parallel RF transmission based MRI technique for highly sensitive detection of amide proton transfer in the human brain at 3T. In: Proc Int Soc Magn Reson Med, p 710

38. Togao O, Hiwatashi A, Keupp J, Yamashita K, Kikuchi K, Yoshiura T, Yoneyama M, Kruiskamp MJ, Sagiyama K, Takahashi M, Honda H (2016) Amide proton transfer imaging of diffuse gliomas: effect of saturation pulse length in parallel transmission-based technique. PLoS One 11:e0155925. https://doi.org/10.1371/journal.pone.0155925